



University of
Massachusetts
Amherst

Effects of Sulfidation and Natural Organic Matter on the Deposition of Silver Nanoparticles

Item Type	Master Projects
Authors	Chen, Yunqui
DOI	10.7275/10w4-z708
Download date	2026-04-10 22:26:54
Link to Item	https://hdl.handle.net/20.500.14394/4829

**Effects of Sulfidation and Natural Organic Matter
on the Deposition of Silver Nanoparticles**

Yunqi Chen

Submitted to the Department of Civil and Environmental Engineering of the University of
Massachusetts in partial fulfillment of the requirements for the degree of

MASTER OF SCIENCE IN ENVIRONMENTAL ENGINEERING

June 2015

Acknowledgements

I would like to gratefully and sincerely thank my advisor, Dr. Boris Lau, for his patience, support, guidance and for encouraging me to pursue my ideas. I would also like to extend my thanks to Dr. Richard Vachet for sitting on my committee as well as other professors in the Department of Civil and Environmental Engineering.

A special thanks to Dr. Kaoru Ikuma for helping me with my experiments and being a constant source of help and guidance.

I would like to thank Dr. Philip Larese-Casanova for his help at Northeastern University.

I would like to thank Charlie Angell for helping me with the aggregation experiments. I would also like to extend my thanks to all my fellow graduate students who have made my time here a memorable one.

Lastly, I would like to thank my friends and family for their love and support.

**EFFECTS OF SULFIDATION AND NATURAL ORGANIC MATTER ON
THE DEPOSITION OF SILVER NANOPARTICLES**

A Masters Project Presented

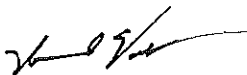
by

YUNQI CHEN


Approved as to style and content by:



Boris Lau, Chairperson



Richard Vachet, Member


Sanjay Arwade
Graduate Program Director
Civil and Environmental Engineering Department

Abstract

Environmental transformation through sulfidation and complexation with natural organic matter (NOM) are two major factors that may affect the fate and transport of silver nanoparticles (AgNPs) in the aquatic systems by changing their dissolution, deposition, and surface properties. To understand the impact of sulfidation and NOM on the aggregation and deposition of AgNPs, a combination of dynamic light scattering and quartz crystal microgravimetry with dissipation monitoring was used. Polyvinylpyrrolidone (PVP)-capped AgNPs that were modified through sulfidation and/or complexed with NOM had a greater extent of deposition than unmodified PVP-AgNPs. Specifically, the deposition extent of sulfidized AgNPs in the presence of NOM, which was the most environmental-relevant form in this study, was 0.5 to almost 3 orders of magnitude greater than unmodified PVP-AgNPs. Bare-silica and NOM-coated substrates were used as a basis for differentiating the effect of substrate on the deposition of PVP-capped AgNPs. Bare-silica substrate was more favorable for the deposition of modified PVP-capped AgNPs (including sulfidized, NOM-complexed, and sulfidized in the presence of NOM) than NOM-coated substrates. Citrate-capped AgNPs were also investigated to study the effect of capping agents on the deposition and surface properties of AgNPs. Since deposition extent implicates the degree of susceptibility to removal by water treatment, citrate-capped AgNPs, which have 6 to 50 orders of magnitude less deposition than PVP-capped AgNPs, are more likely to persist in the aquatic environments.

Table of Contents

Acknowledgements	i
Abstract.....	iii
1. Introduction	1
2. Materials and Methods	3
2.1 Preparation and Characterization of Nanoparticle Suspensions	3
2.2 QCM-D and Substrate Preparation.....	5
2.3 Dissolution of AgNPs	6
3. Results and Discussions	7
3.1 Characteristics of AgNPs.....	7
3.2 Deposition of PVP-capped AgNPs.....	8
3.3 Comparison among three substrates.....	11
3.4 Dissolution of AgNPs	12
3.5 Effect of Capping Ligands on AgNP Deposition	13
3.6 Environmental Implications.....	13
References	14
List of Figures and Tables	17
Figure 1. Size distribution of PVP-capped AgNPs at 5 mM NaNO ₃ and pH = 7.0 ± 0.2.....	17
Table 1. Characteristics of PVP-capped AgNPs at 5 mM NaNO ₃ and pH = 7.0 ± 0.2	18
Figure 2. The hydrodynamic diameter of 4 types of AgNPs	19
Table 2. Characteristics of PVP-AgNPs and citrate-AgNPs at 5 mM NaNO ₃ and pH = 7.0 ± 0.2	20
Figure 3. Zeta Potential of 4 types of PVP-capped AgNPs at 5 mM NaNO ₃ and pH = 7.0 ± 0.2 and 3 substrates (bare-silica, HA-coated and FA-coated) at pH = 8.0 ± 0.2	21
Figure 4. Size distribution of PVP-AgNPs and citrate-AgNPs	22
Table 3. Extent of silver ion dissolution at 5 mM NaNO ₃ and pH = 7.0 ± 0.2.....	23
Figure 5. Chemical structure of PVP and citrate.....	24
Figure 8. Deposition Extent of PVP and Citrate-coated AgNPs on FA coated substrates at 5 mM NaNO ₃ and pH 7.0 ± 0.2. Error bars are standard errors.	27
Supplementary Information	28

1. Introduction

Silver nanoparticles (AgNPs) have been incorporated into more than 400 consumer products (~27% of over 1800 products that contain nanomaterials) due to their potent antimicrobial applications.^{1,2} Because of their broad applications, it is likely that different forms (ions, particles, or aggregates³) of silver (Ag) will be released into the environment throughout the different stages of its life cycle. There are concerns about the fate,^{3,4} transport,⁴⁻⁶ bioavailability^{1,7,8} and toxicity⁹⁻¹² associated with the release of AgNPs. Once different species of Ag enter the aquatic environment, they are likely to interact with organic ligands,^{13,14} and be transformed through photoreduction,^{1,15} oxidation,^{16,17} and sulfidation.^{4,6,16} The environmental behaviors of different types of transformed AgNPs are not fully understood and are dependent on the water chemistry conditions and the properties of AgNPs. Dissolution¹⁸ and sulfidation¹⁷ have been shown to significantly impact the stability and toxicity of AgNPs.

Most of the sulfidation conditions in natural and engineered water systems will partially sulfidize AgNPs.^{4,6} For example, AgNPs were partially sulfidized in anaerobic zones of the wastewater treatment plants (WWTPs) at a Na₂S concentration of ~1 mM.⁶ Dale et al. have shown that the extent of sulfidation for AgNPs at the effluent of a WWTP is expected to be around 85%.¹⁶ Furthermore, Kaegi et al.⁴ suggested that citrate-AgNPs in raw wastewater were 15% sulfidized after 5 hours. They have also shown that the degree of sulfidation is dependent on the size of AgNPs. After 24 hours of sulfidation, more than 95% of the 10 nm AgNPs were sulfidized while only 10% of the 100 nm AgNPs were sulfidized.⁴ Polyvinylpyrrolidone (PVP) is a common coating used in the synthesis of nanoparticles (NPs) to prevent aggregation through steric

stabilization. Surface charge and dissolution rate of PVP-capped AgNPs (39 nm) were found to be significantly different after sulfidation.¹⁹ It has been shown that a S/Ag ratio as low as 0.019 can reduce the dissolution from 20 ppm to 3 ppm in 30 days by forming Ag₂S ($K_{sp} = 10^{-50}$).¹⁹⁻²¹ Subsequently, NPs of Ag₂S will limit 24-hours toxicity by inhibiting the release of Ag ions. However, nanoparticulate Ag₂S can exert toxicity effects over 2 weeks through direct accumulation in terrestrial plant tissues.⁸ Overall, it is important to study the transformation of AgNPs in aquatic environments because partial sulfidation would change the surface properties of AgNPs and form new species (e.g., Ag₂S), and the transformation may affect their subsequent fate and transport.

Due to the complex environments in WWTPs, sewers and other aquatic systems, partially sulfidized AgNPs are likely to have further interactions with NOM or microorganisms. It has been shown that AgNPs can complex with NOM, which is ubiquitous in aquatic systems.^{13,14,22} For example, Furman et al. have shown that citrate-capped AgNP-NOM complexes have different extent and kinetics of aggregation and deposition when compared to citrate-AgNPs (49 nm) and may potentially influence subsequent fate of AgNPs.¹³ Therefore, it is important to understand the fate and transport of partially sulfidized AgNPs in the presence of NOM. To our knowledge, only Deonarine et al. and Kent et al. have studied the sulfidation of NPs in the presence of NOM, which is a more environmentally-relevant condition.^{6,23} Functionalization of NP surface with organic ligands is another important factor in controlling toxicity and stability of AgNPs. PVP and citrate are commonly used as capping for AgNPs. Previous studies have shown that part of the capping agent were lost during sulfidation,^{19,24} which may affect their further interactions with NOM.

The goal of this study is to determine if the different forms of AgNPs (with and without sulfidation) will interact differently with NOM in aquatic environments. Those modified AgNPs may possess different properties (e.g., size and charge), which will subsequently cause differences in their deposition under controlled laboratory conditions. To mimic sand in natural water as an environmentally relevant surface, silica substrates were coated with NOM. The aggregation and deposition kinetics of partially sulfidized AgNPs with and without NOM were determined by utilizing dynamic light scattering (DLS) and quartz crystal microgravimetry with dissipation monitoring (QCM-D). In addition, the dissolution of AgNPs was analyzed with inductively coupled plasma mass spectrometry (ICP-MS).

2. Materials and Methods

2.1 Preparation and Characterization of Nanoparticle Suspensions

PVP-capped AgNPs and citrate-capped AgNPs were purchased from NanoComposix (San Diego, CA) with a reported diameter of 50 nm as determined by manufacturer using transmission electron microscopy. The molecular weight of PVP and citrate that used in this study are 40 kDa and 189 g/mol respectively. All solutions/suspensions were prepared using Milli-Q water with a solution chemistry of 5 mM NaNO₃ and 1mM phosphate buffer with a pH adjusted to 7.0 ± 0.2 using 1 M HCl. The background solution was filtered with a 0.2µm nylon filter before use.

Two types of NOM, Suwannee River Fulvic Acid Standard II (FA) and Suwannee River Humic Acid Standard II (HA), were purchased from the International Humic Substances Society (IHSS, www.humicsubstances.org). The NOM stock solutions (50 mg L⁻¹) were prepared by dissolving NOM powder in the background solution with a pH of 7.0 ± 0.2. Dissolved organic carbon

(DOC) concentrations were determined using a Shimadzu TOC-VCPH Analyzer (Kyoto, Japan). The NOM stock solutions (19 mg L^{-1} DOC) were stored in the dark at $4 \text{ }^\circ\text{C}$. There were four types of PVP-capped AgNPs (10 mg L^{-1}) in this study: (a) AgNPs that received no further treatment (PVP-AgNPs), (b) AgNPs that were mixed with NOM solution to represent the initial form of AgNPs in surface water (AgNPs-HA), (c) AgNPs that have been partly sulfidized in the absence of NOM, as a model of “transformed species” (S-AgNPs), and (d) AgNPs that have received partial sulfidation in the presence of NOM, to mimic the reducing condition such as those encountered in wastewater treatment (S-AgNPs-HA). In addition, 10 mg L^{-1} AgNO_3 was used to represent ionic Ag. The sulfidation procedures described by Levard et al. and a S/Ag ratio of 1.079 were used in this study.¹⁹ With the exception of PVP-AgNPs, all suspensions of AgNPs were stored in the dark for 24 h before centrifugation at 9000 G for 20 min twice to remove excess Na_2S and unbound NOM. Pellets were then resuspended in background solution for further QCM-D and DLS measurements. The same sulfidation procedure was also performed on citrate-AgNPs. Ag_2S -HA and Ag_2S were prepared by mixing 4 mM AgNO_3 with 2 mM Na_2S in the presence and absence of HA. All solutions were purged with nitrogen gas before mixing. For Ag_2S -HA, suspension was centrifuged at 9000 G for 20 min to remove unbound HA and pellets were then resuspended in background solution for further ZP and DLS measurements.

The hydrodynamic diameter (D_H) and zeta potential (ZP) of AgNPs were monitored over time at $25 \text{ }^\circ\text{C}$ by DLS and electrophoretic mobility measurements using a Malvern Zetasizer NS (Worcestershire, U.K.). The observed growth rate of AgNPs, (dD_H/dt), were calculated from the change in the average D_H of the AgNPs over 90 minutes and derived from a linear least-squares regression equation. The ZP was estimated from electrophoretic mobility using the Smoluchowski approximation. The critical coagulation concentrations (CCCs) of PVP-capped

AgNPs were also determined through determination of aggregation kinetics using DLS. The aggregation rate constant, k , can be obtained from the rate of D_H change with time as measured by time-resolved DLS. The attachment efficiency, α , is used to quantify the aggregation kinetics of AgNPs. It is calculated by normalizing the aggregation rate constant obtained in the solution of interest to the rate constant obtained under favorable aggregation conditions (k_{fast}); therefore, $\alpha = k/k_{fast}$. CCC is reached when $\alpha = 1$. All D_H measurements were conducted at a scattering angle of 173° and performed over 30 min to 2 h to achieve a large enough ΔD_H (up to 6 times of initial D_H) for accurate derivation of aggregation kinetics. Triplicate measurements were performed.

2.2 QCM-D and Substrate Preparation

Real-time deposition kinetics and extent for four types of AgNPs were quantitatively determined by QCM-D at 25 ± 0.02 °C. QCM-D resolves mass differences with high sensitivity (ng/cm^2) using the piezoelectric property of quartz.²⁵ The mass change on the surface of the quartz (Δm) can be related to the change in oscillation frequency (Δf) according to the Sauerbrey relation,²⁶

$$\Delta m = - C \Delta f / n$$

where C is the sensitivity constant of the crystal ($17.7 \text{ ng cm}^2 / \text{Hz}$), and n is the number of the overtone.

Silica-coated quartz crystals (QSX 303, Q-Sense AB, Gothenburg, Sweden) were used as substrates for each experiment. Silica substrates were soaked in sodium dodecyl sulfate solution overnight, then rinsed with Milli-Q water, dried with nitrogen gas and placed in an UV/ozone cleaner for 20 min to remove any trace organics before each experiment. All solutions/suspensions were well mixed and injected into the QCM-D flow module at a rate of 0.1

mL min⁻¹. The silica substrates were equilibrated with the background solution for 30 min to obtain baseline conditions. Modifications of silica substrate were performed as described in Furman et al.¹³ First, cationic poly-L-lysine (PLL) (0.1 g mL⁻¹) was adsorbed on the silica substrate to establish a positively charged surface as an electrostatically favorable condition for later adsorption of NOM. The PLL layer was then rinsed with background solution for 10 min and exposed to a 50 mg L⁻¹ NOM (19 mg L⁻¹ DOC) solution. After the adsorption of NOM onto PLL-coated silica reached saturation ($\Delta f / \Delta t \leq 0.26$ Hz/min), the NOM layer was rinsed with background solution to remove any unbound NOM. Suspensions of AgNPs (10 mg L⁻¹) were then passed over the substrate until saturation.

The observed rate of AgNP deposition (dm/dt) was calculated from the time taken to reach the first 50% deposition where the relationship between deposition and time were linear ($R^2 > 0.98$). With the best signal-to-noise ratio, Δf obtained from the third overtone are presented in this study.

2.3 Dissolution of AgNPs

A Perkin-Elmer ELAN 9000 inductively coupled plasma mass spectrometer (ICP-MS) (Waltham, MA) was used to quantify the concentration of dissolved Ag during the deposition experiments. After the duration of a QCM run, AgNPs were removed by passing through an Amicon Ultra-4 centrifugal filter (with a molecular weight cutoff of 3000 kDa) at 8000 G for 30 min and the filtrates were diluted and analyzed by ICP-MS.

3. Results and Discussions

3.1 Characteristics of AgNPs

PVP-capped AgNPs. DLS experiments were performed to quantify the D_H and CCC (Table 1) of four types of PVP-capped AgNPs. Figure 1 is an example of the size distribution for PVP-capped AgNPs. The size distribution of PVP-capped AgNPs became broader after sulfidation with sizes ranging from 25-190 nm to 25-300 nm. The average peak values of D_H (> 30 measurements) from the size distributions were reported in Table 1. There was no observable aggregation over 90 minutes for all four types of AgNPs (Figure 2). The D_H growth rates of AgNPs were all below $0.05 \pm 0.01 \text{ nm min}^{-1}$. This indicated that there was no observable aggregation during the deposition of AgNPs. CCC was used to compare the relative stability of the four types of AgNPs. The CCC of PVP-AgNPs is greater than 3000 mM due to the steric stabilization of PVP capping. Surface modification of AgNPs, including sulfidation and interaction with NOM, decreased their CCCs. Specifically, S-AgNPs has the lowest CCC of 400 mM (Table 1), which means that S-AgNPs was the least stable among the four types of AgNPs. Reduced steric repulsion due to the partial loss of PVP may explain why S-AgNPs was less stable. The adsorption of HA on the NP surface makes AgNPs-HA less stable than PVP-AgNPs. The CCC of S-AgNPs-HA (1300 mM) was greater than S-AgNPs (400 mM) and AgNPs-HA (500 mM). This suggests that the most environmental-relevant form, S-AgNPs-HA, is the most stable form among the three modified AgNPs in this study.

For AgNPs coated with PVP, the ZPs of PVP-AgNPs and AgNPs-HA were found to be less negative than the ZPs of S-AgNPs and S-AgNPs-HA ($p < 0.05$) (Figure 3). PVP is uncharged but Ag_2S (-49.3 mV) and Ag_2S -HA (-19.9 mV) are both negatively charged (Table 2). Stronger

electrostatic repulsion was expected after partial loss of PVP, possibly due to the formation of Ag₂S. Consistently, more negative ZP values were observed when partial PVP was removed, which is caused by sulfidation in this case.

Citrate-AgNPs. Citrate-AgNPs were also investigated to study the effect of capping on the deposition of AgNPs. Citrate is a common capping used to maintain particle stability through electrostatic repulsion. Citrate-AgNPs were also stable under experimental conditions (5 mM NaNO₃ and pH 7.0 ± 0.2) for 90 min. The average peak values of D_H (> 30 measurements) were reported in Table 2. Figure 4 indicates that the size distribution became broader after sulfidation for both PVP- and citrate-capped AgNPs. However, unlike PVP-capped AgNPs, the ZP of citrate-AgNPs became less negative after sulfidation (Table 2). Badawy et al.²⁷ have shown that citrate-capped AgNPs are more negatively charged than AgNPs without capping (H₂-AgNPs), because the carboxyl groups of the citrate on NP surface can induce negative surface charge (Figure 5). Baalousha et al.²⁴ suggested that sulfidation could cause partial loss of citrate capping on AgNPs. Therefore, the partial loss of negatively charged citrate capping could explain why the ZP of citrate-S-AgNPs-HA is less negative than citrate-AgNPs. Furthermore, the ZP of Ag₂S-HA (-19.9 mV) is significantly less than the ZP of citrate-AgNPs (-41.1 mV), so the formation of Ag₂S-HA could also be a reason why citrate-S-AgNPs-HA is less negatively charged than citrate-AgNPs.

3.2 Deposition of PVP-capped AgNPs

The AgNP deposition kinetic was presented in terms of the deposition extent and the deposition rate. Total deposition extent (ng cm⁻²) and frequency shift (Hz) were estimated using the Sauerbrey equation and quantified by QCM-D, respectively (Figure 6). Three substrates (bare-

silica, HA- or FA-coated) were prepared using a procedure described by Furman et al¹³, and they were all negatively charged according to the ZPs (-32 mV for bare-silica, -29 mV for HA and -44 mV for FA) presented in their study. The four types of AgNPs were also negatively charged (Figure 3). Although negatively charged substrates may induce electrostatic repulsion to prevent the deposition of negatively charged AgNPs, AgNPs may still deposit on the substrates through non-electrostatic forces such as hydrophobic interaction. There were 12 deposition conditions based on four types of AgNPs and three kinds of substrates. One-tailed and two-tailed student's t tests were performed on the deposition data (Tables S1-S4). Significant differences were reported when a p-value is < 0.05.

PVP-AgNPs vs. AgNPs-HA. The deposition extent of PVP-AgNPs was 61% to 97% less than the other three modified AgNPs ($p < 0.05$) on all three substrates (bare-silica, HA or FA) (Figure 6). PVP-AgNPs are sterically stabilized by the PVP molecules. Therefore, the less deposition extent of PVP-AgNPs on substrate surfaces was probably due to the steric repulsion force exerted by PVP. Specifically, PVP-AgNPs deposited 81% to 85% less than AgNPs-HA on all three substrates. Furman et al.¹³ made similar observations when they examined the deposition of citrate-capped AgNPs and AgNPs-HA on bare-silica and FA-coated substrates. Previous studies have shown that NOM can alter NP surfaces not only through adsorption but also by ligand exchange.^{28,29} The adsorption and/or ligand exchange of HA on the surface of AgNPs could potentially reduce steric repulsion by removing the PVP coating and/or altering its molecular orientation. The higher deposition extent of AgNPs-HA compared to PVP-AgNPs on all substrates suggests that the adsorption and ligand-exchange of HA on the surface of NPs may reduce steric repulsion and subsequently enhance the deposition extent of AgNPs-HA.

PVP-AgNPs vs. S-AgNPs. Levard et al.¹⁹ have shown that part of the PVP coating was lost

during sulfidation, and the amount of PVP lost is proportional to the S/Ag ratio. With a S/Ag ratio of 1.079, about 43% of PVP was lost after sulfidation.¹⁹ AgNPs were not completely coated with PVP after sulfidation, resulting in a potential reduction of steric repulsion exerted by the AgNPs. When compared with PVP-AgNPs, S-AgNPs (the less sterically stable form) has 2 to 6 times higher extent of deposition (Figure 6) on all three substrates. However, the ZPs of S-AgNPs was more negative than PVP-AgNPs ($p < 0.05$). The QCM deposition and ZP results indicated that electrostatic force was less dominant than steric repulsion in controlling the deposition extent of S-AgNPs.

S-AgNPs vs. S-AgNPs-HA. The most environmentally-relevant form of AgNPs, S-AgNPs-HA, had the greatest extent of deposition among the four types of AgNPs on bare-silica and FA-coated substrates. After the partial loss of PVP, there may be available binding sites for HA to adsorb onto the core surface of AgNPs and/or to complex with PVP that remained on the NP surface. In contrast, on HA-coated substrates, S-AgNPs-HA did not have the greatest extent of deposition among the four types of AgNPs. In fact, the extent of S-AgNPs-HA deposition ($425 \pm 64 \text{ ng cm}^{-2}$) was not statistically different than S-AgNPs ($466 \pm 94 \text{ ng cm}^{-2}$) on the HA-coated substrate ($p > 0.05$). There are at least two possible explanations that may account these results. Firstly, HA is known to be hydrophobic^{30,31} and HA-coated substrate is more hydrophobic than the other 2 substrates.¹³ The deposition results suggested that higher hydrophobicity of adsorbed HA on the substrate could lead to greater electrosteric (i.e., combination of electrostatic and steric) repulsion between AgNPs and HA-coated substrate and resulted in a smaller extent of deposition. Furman et al.¹³ also observed that the adsorbed HA on PLL-coated silica substrate induced electrosteric repulsion to prevent the subsequent deposition of citrate-capped AgNPs-HA. Secondly, previous studies have suggested that similar surface components would decrease

the affinity between NPs and substrates,³² such as the case where HA was present on the S-AgNPs-HA and the HA-coated substrate. Therefore, the similar surfaces on the AgNPs and the substrate could potentially be a reason why S-AgNPs-HA did not achieve the greatest deposition on HA-coated substrate.

When comparisons were made between AgNPs with (AgNPs-HA and S-AgNPs-HA) and without HA (PVP-AgNPs and S-AgNPs), AgNPs with HA had greater deposition extent in a few conditions. Specifically, on the FA substrate, there was a significantly greater deposition extent of AgNPs-HA and S-AgNPs-HA of $377 \pm 6 \text{ ng cm}^{-2}$ and $540 \pm 44 \text{ ng cm}^{-2}$, respectively, than PVP-AgNPs and S-AgNPs of $69 \pm 6 \text{ ng cm}^{-2}$ and $177 \pm 24 \text{ ng cm}^{-2}$, respectively (Figure 6b). Regardless of substrates, modified AgNPs (AgNPs-HA, S-AgNPs, S-AgNPs-HA) have more deposition extent than PVP-AgNPs. Especially, the deposition extent of the most environmentally-relevant form, S-AgNPs-HA, was $\geq 425 \pm 63 \text{ ng cm}^{-2}$. This indicates that the AgNPs with environmentally-relevant forms might be more susceptible to removal by natural (e.g., hyporheic exchange) and engineered water environment (e.g., sand filtration).

3.3 Comparison among three substrates

The extents of PVP-AgNP deposition on bare-silica, HA- and FA-coated substrates were $99 \pm 15 \text{ ng cm}^{-2}$, $87 \pm 6 \text{ ng cm}^{-2}$ and $69 \pm 6 \text{ ng cm}^{-2}$, respectively. T-test results showed that they were not significantly different from each other ($p > 0.05$). However, three other modified AgNPs (AgNPs-HA, S-AgNPs and S-AgNPs-HA) deposited differently on the three different substrates. The three modified AgNPs have the greatest extent of deposition on the bare-silica substrate (Figure 6). Specifically, S-AgNPs-HA has a significantly greater deposition extent ($2930 \pm 37 \text{ ng cm}^{-2}$) on the bare-silica substrate than the other two substrates ($540 \pm 44 \text{ ng cm}^{-2}$ for FA and 425 ± 64

ng cm⁻² for HA). Similar trends were also observed on the rate of deposition as AgNPs deposited faster on the bare-silica substrate than the other two NOM-coated substrates (Figure 7). Both the extent and rate of AgNP deposition indicate that the bare-silica substrate possessed more favorable conditions for the deposition of modified AgNPs than NOM-coated substrates.

When comparisons were made on the deposition of AgNPs between HA- and FA-coated substrates, similar deposition dynamics as Furman et al.¹³ was observed that the amount of AgNPs deposited was not significantly different between the FA-coated and HA-coated substrates ($p > 0.05$). HA and FA are the two fractions of NOM and HA is known to be more hydrophobic and heterogeneous (both spatially and chemically) than FA.^{30,31} Although the deposition extent of AgNPs-HA and S-AgNPs on FA substrate were found to be less than the deposition on HA substrate ($p < 0.05$), the other two types of NPs (PVP-AgNPs and S-AgNPs-HA) showed no significant difference in deposition between HA- and FA-coated substrates. In addition, the deposition rate of all four types of AgNPs between the HA and FA substrates (Figure 7 b and c) were also not statistically different from each other ($p > 0.05$). Overall, the substrate modification by different fractions of NOM did not significantly affect the rate and extent of deposition of AgNPs.

3.4 Dissolution of AgNPs

ICP-MS experiments were performed to evaluate the dissolution of PVP-capped AgNPs during QCM experiments. A range of dissolution durations (0.5 hr to 5 hr) were used to reflect the time taken for each type of AgNPs to deposit on the substrate before saturation ($\Delta f / \Delta t \leq 0.26$ Hz/min) was reached. Table 3 shows that 0.05% of silver was dissolved in 30 min for PVP-AgNPs and the dissolution extents of modified AgNPs were even lower. These results are in agreement with

previous studies that sulfidation could significantly reduce the dissolution rate of AgNPs by forming Ag₂S ($K_{sp} = 10^{-50}$).¹⁹⁻²¹ Overall, the ICP-MS results indicate that the release of silver ions during QCM experiments was insignificant and the frequency shift measured by QCM was caused by AgNPs. The dissolution extents after a week were not significantly different compared to samples with <5 hr of dissolution.

3.5 Effect of Capping Ligands on AgNP Deposition

QCM experiments were also performed on citrate-capped AgNP to study the effect of capping ligands on the deposition of AgNPs, which could potentially affect their subsequent fate and transport in environments. Previous study have suggested that capping agents might be an important factor in controlling AgNP toxicity.³³ Figure 8 shows that there was no observable deposition of both citrate-AgNPs and citrate-S-AgNPs-HA. This indicates that citrate-AgNPs are more difficult to be immobilized during water treatment (e.g., sand filtration). Therefore, under the tested conditions of this study, citrate-AgNPs are relatively easier to persist than PVP-capped AgNP.

3.6 Environmental Implications

Sulfidation and NOM are two major factors that could contribute to changes in aggregation and deposition kinetics of AgNPs and further affect their fate and transport in wastewater and natural water systems. This study highlights the importance of environmental transformation on the deposition of AgNPs. The deposition results showed that AgNPs in an environmentally-relevant form (S-AgNPs-HA) is potentially more susceptible to removal by granular media filtration. Another notable conclusion of this research is that bare-silica substrates possess more favorable conditions for modified AgNP deposition than NOM-coated substrates.

References

- (1) Chaloupka, K.; Malam, Y.; Seifalian, A. M. Nanosilver as a new generation of nanoproduct in biomedical applications. *Trends Biotechnol.* **2010**, *28*, 580–588.
- (2) Woodrow Wilson International center for Scholar. Nano-Technology Consumer Products Inventory <http://www.nanotechproject.org/cpi/browse/nanomaterials/silver-nanoparticle/> (accessed Feb 20, 2015).
- (3) Benn, T. M.; Westerhoff, P. Nanoparticle silver released into water from commercially available sock fabrics. *Environ. Sci. Technol.* **2008**, *42*, 4133–4139.
- (4) Kaegi, R.; Voegelin, A.; Ort, C.; Sinnet, B.; Thalmann, B.; Krismer, J.; Hagendorfer, H.; Elumelu, M.; Mueller, E. Fate and transformation of silver nanoparticles in urban wastewater systems. *Water Res.* **2013**, *47*, 3866–3877.
- (5) El Badawy, A. M.; Hassan, A. A.; Scheckel, K. G.; Suidan, M. T.; Tolaymat, T. M. Key factors controlling the transport of silver nanoparticles in porous media. *Environ. Sci. Technol.* **2013**, *47*, 4039–4045.
- (6) Kent, R. D.; Oser, J. G.; Vikesland, P. J. Controlled evaluation of silver nanoparticle sulfidation in a full-scale wastewater treatment plant. *Environ. Sci. Technol.* **2014**, *48*, 8564–8572.
- (7) Fabrega, J.; Luoma, S. N.; Tyler, C. R.; Galloway, T. S.; Lead, J. R. Silver nanoparticles: Behaviour and effects in the aquatic environment. *Environment International*, 2011, *37*, 517–531.
- (8) Wang, P.; Menzies, N. W.; Lombi, E.; Sekine, R.; Blamey, F. P. C.; Hernandez-Soriano, M. C.; Cheng, M.; Kappen, P.; Peijnenburg, W. J. G. M.; Tang, C.; et al. Silver sulfide nanoparticles (Ag₂S-NPs) are taken up by plants and are phytotoxic. *Nanotoxicology* **2015**, *5390*, 1–9.
- (9) Asharani, P. V.; Lian Wu, Y.; Gong, Z.; Valiyaveetil, S. Toxicity of silver nanoparticles in zebrafish models. *Nanotechnology* **2008**, *19*, 255102.
- (10) Levard, C.; Hotze, E. M.; Lowry, G. V.; Brown, G. E. Environmental transformations of silver nanoparticles: impact on stability and toxicity. *Environ. Sci. Technol.* **2012**, *46*, 6900–6914.
- (11) Sondi, I.; Salopek-Sondi, B. Silver nanoparticles as antimicrobial agent: a case study on *E. coli* as a model for Gram-negative bacteria. *J. Colloid Interface Sci.* **2004**, *275*, 177–182.
- (12) Lu, W.; Senapati, D.; Wang, S.; Tovmachenko, O.; Singh, A. K.; Yu, H.; Ray, P. C. Effect of surface coating on the toxicity of silver nanomaterials on human skin keratinocytes. *Chem. Phys. Lett.* **2010**, *487*, 92–96.

- (13) Furman, O.; Usenko, S.; Lau, B. L. T. Relative importance of the humic and fulvic fractions of natural organic matter in the aggregation and deposition of silver nanoparticles. *Environ. Sci. Technol.* **2013**, *47*, 1349–1356.
- (14) Gao, J.; Powers, K.; Wang, Y.; Zhou, H.; Roberts, S. M.; Moudgil, B. M.; Koopman, B.; Barber, D. S. Influence of Suwannee River humic acid on particle properties and toxicity of silver nanoparticles. *Chemosphere* **2012**, *89*, 96–101.
- (15) Yin, Y.; Shen, M.; Zhou, X.; Yu, S.; Chao, J.; Liu, J.; Jiang, G. Photoreduction and stabilization capability of molecular weight fractionated natural organic matter in transformation of silver ion to metallic nanoparticle. *Environ. Sci. Technol.* **2014**, *48*, 9366–9373.
- (16) Dale, A. L.; Lowry, G. V.; Casman, E. a. Modeling Nanosilver Transformations in Freshwater Sediments Modeling Nanosilver Transformations in Freshwater Sediments Center for Environmental Implications of Nanotechnology. *Environ. Sci. Technol.* **2013**, *Just Accep.*
- (17) Liu, J.; Pennell, K. G.; Hurt, R. H. Kinetics and mechanisms of nanosilver oxysulfidation. *Environ. Sci. Technol.* **2011**, *45*, 7345–7353.
- (18) Ma, R.; Levard, C.; Marinakos, S. M.; Cheng, Y.; Liu, J.; Michel, F. M.; Brown, G. E.; Lowry, G. V. Size-controlled dissolution of organic-coated silver nanoparticles. *Environ. Sci. Technol.* **2012**, *46*, 752–759.
- (19) Levard, C.; Reinsch, B. C.; Michel, F. M.; Oumahi, C.; Lowry, G. V.; Brown, G. E. Sulfidation processes of PVP-coated silver nanoparticles in aqueous solution: Impact on dissolution rate. *Environ. Sci. Technol.* **2011**, *45*, 5260–5266.
- (20) Ma, D.; Hu, X.; Zhou, H.; Zhang, J.; Qian, Y. Shape-controlled synthesis and formation mechanism of nanoparticles-assembled Ag₂S nanorods and nanotubes. *J. Cryst. Growth* **2007**, *304*, 163–168.
- (21) Graedel, T. E. Corrosion Mechanisms for Silver Exposed to the Atmosphere. *J. Electrochem. Soc.* **1992**, *139*, 1963.
- (22) Yang, X.; Lin, S.; Wiesner, M. R. Influence of natural organic matter on transport and retention of polymer coated silver nanoparticles in porous media. *J. Hazard. Mater.* **2014**, *264*, 161–168.
- (23) Deonaraine, A.; Hsu-Kim, H. Precipitation of mercuric sulfide nanoparticles in NOM-containing water: Implications for the natural environment. *Environ. Sci. Technol.* **2009**, *43*, 2368–2373.
- (24) Baalousha, M.; Arkill, K. P.; Romer, I.; Palmer, R. E.; Lead, J. R. Transformations of citrate and Tween coated silver nanoparticles reacted with Na₂S. **2015**, *502*, 344–353.

- (25) Feiler, A. A.; Sahlholm, A.; Sandberg, T.; Caldwell, K. D. Adsorption and viscoelastic properties of fractionated mucin (BSM) and bovine serum albumin (BSA) studied with quartz crystal microbalance (QCM-D). *J. Colloid Interface Sci.* **2007**, *315*, 475–481.
- (26) Rodahl, M.; Höök, F.; Krozer, A.; Brzezinski, P.; Kasemo, B. Quartz crystal microbalance setup for frequency and Q-factor measurements in gaseous and liquid environments. *Rev. Sci. Instrum.* **1995**, *66*, 3924–3930.
- (27) Badawy, a. M. E.; Luxton, T. P.; Silva, R. G.; Scheckel, K. G.; Suidan, M. T.; Tolaymat, T. M. Impact of environmental conditions (pH, ionic strength, and electrolyte type) on the surface charge and aggregation of silver nanoparticle suspensions. *Environ. Sci. Technol.* **2010**, *44*, 1260–1266.
- (28) Division, E. S.; Ridge, O. Competitive adsorption, displacement, and transport of organic matter on iron oxide: I. Competitive adsorption. **2008**, *60*, 1943–1950.
- (29) Gondikas, A. P.; Morris, A.; Reinsch, B. C.; Marinakos, S. M.; Lowry, G. V.; Hsu-Kim, H. Cysteine-induced modifications of zero-valent silver nanomaterials: Implications for particle surface chemistry, aggregation, dissolution, and silver speciation. *Environ. Sci. Technol.* **2012**, *46*, 7037–7045.
- (30) Baalousha, M.; Motelica-Heino, M.; Coustumer, P. Le. Conformation and size of humic substances: Effects of major cation concentration and type, pH, salinity, and residence time. *Colloids Surfaces A Physicochem. Eng. Asp.* **2006**, *272*, 48–55.
- (31) Ritchie, J. D.; Michael Perdue, E. Proton-binding study of standard and reference fulvic acids, humic acids, and natural organic matter. *Geochim. Cosmochim. Acta* **2003**, *67*, 85–93.
- (32) Lin, S.; Cheng, Y.; Liu, J.; Wiesner, M. R. Polymeric coatings on silver nanoparticles hinder autoaggregation but enhance attachment to uncoated surfaces. *Langmuir* **2012**, *28*, 4178–4186.
- (33) El Badawy, A. M.; Silva, R. G.; Morris, B.; Scheckel, K. G.; Suidan, M. T.; Tolaymat, T. M. Surface charge-dependent toxicity of silver nanoparticles. *Environ. Sci. Technol.* **2011**, *45*, 283–287.

List of Figures and Tables

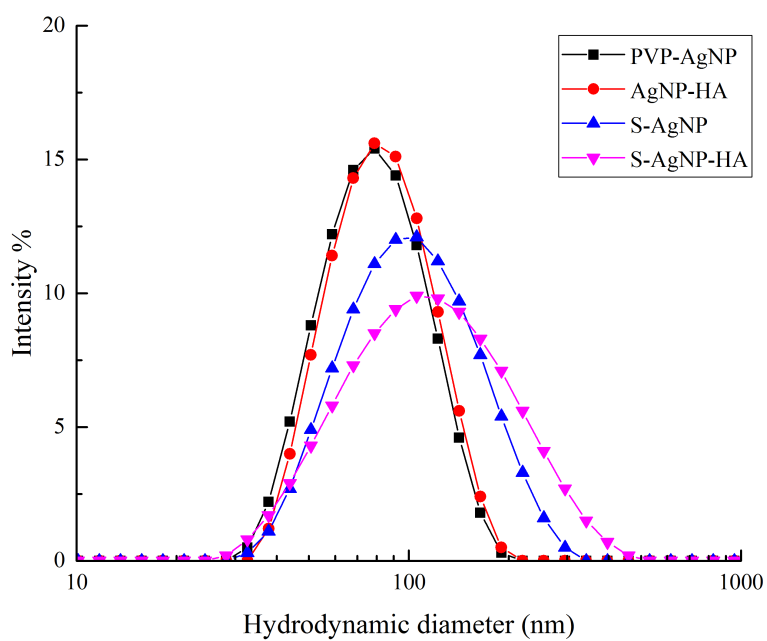


Figure 1. Size distribution of PVP-capped AgNPs at 5 mM NaNO₃ and pH = 7.0 ± 0.2

Table 1. Characteristics of PVP-capped AgNPs at 5 mM NaNO₃ and pH = 7.0 ± 0.2

AgNPs	D _H ^a (nm)	CCC (mM NaNO ₃)
PVP-AgNPs	81.0 ± 0.5	> 3000
AgNPs-HA	83.4 ± 1.0	500
S-AgNPs	108.12 ± 16.2	400
S-AgNPs-HA	111.22 ± 14.3	1300

^aMean ± St Deviation, N = 3.

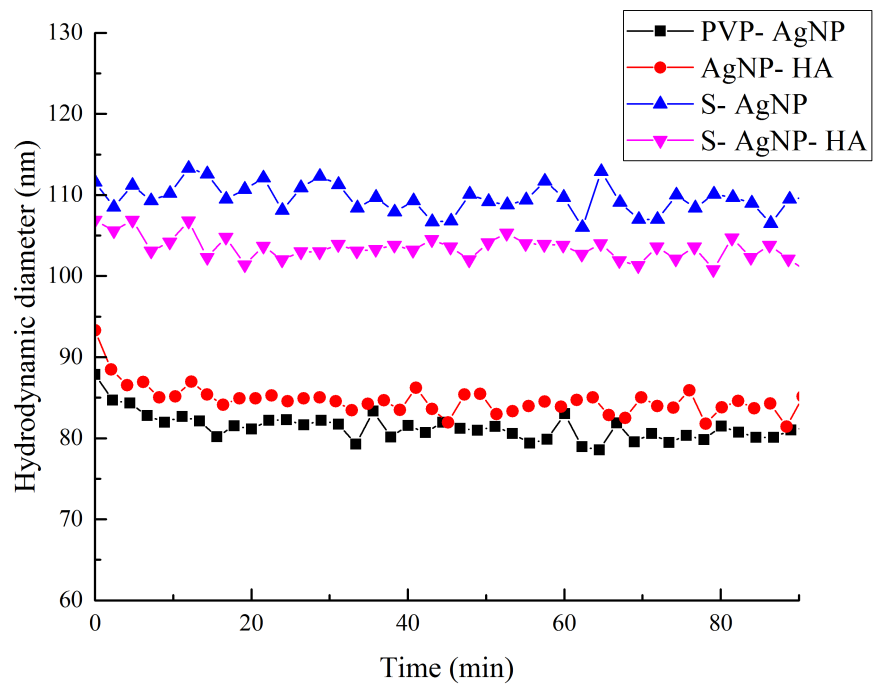


Figure 2. The hydrodynamic diameter of 4 types of AgNPs at 5 mM NaNO₃ and pH = 7.0 ± 0.2

Table 1. Characteristics of PVP-AgNPs and citrate-AgNPs at 5 mM NaNO₃ and pH = 7.0 ± 0.2

AgNPs	D _H ^a (nm)	Zeta potential ^b (mV)
PVP-AgNPs	81.0 ± 0.5	-21.4 ± 2.4
Citrate-AgNP	57.9 ± 1.0	-41.1 ± 3.0
PVP-S-AgNPs-HA	111.2 ± 14.3	-29.2 ± 5.1
Citrate-S-AgNPs-HA	65.7 ± 1.0	-33.9 ± 0.7
Ag ₂ S	76.2 ± 3.1	-49.3 ± 0.9
Ag ₂ S-HA	32.8 ± 1.7	-19.9 ± 1.5

^{a,b}Mean ± St Deviation, N = 3.

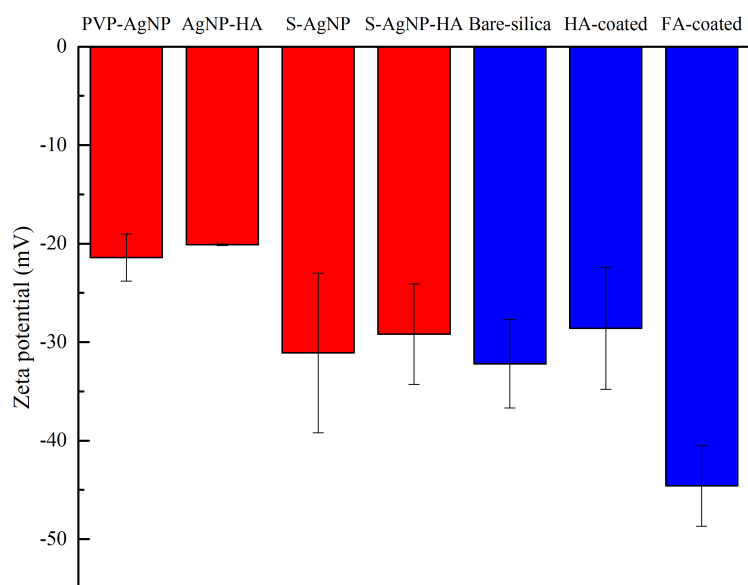


Figure 3. Zeta Potential of 4 types of PVP-capped AgNPs at 5 mM NaNO₃ and pH = 7.0 ± 0.2 and 3 substrates (bare-silica, HA-coated and FA-coated) at pH = 8.0 ± 0.2

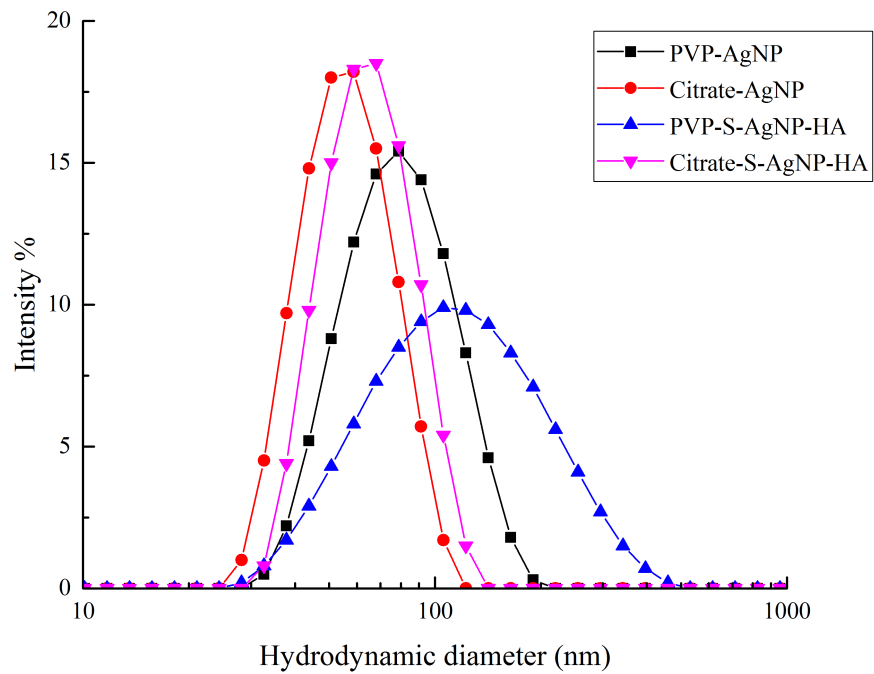
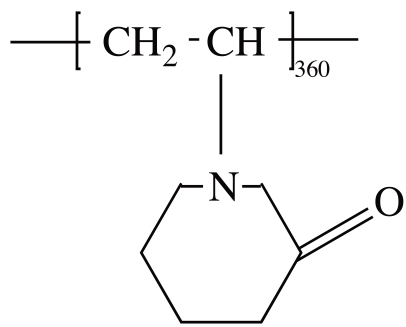


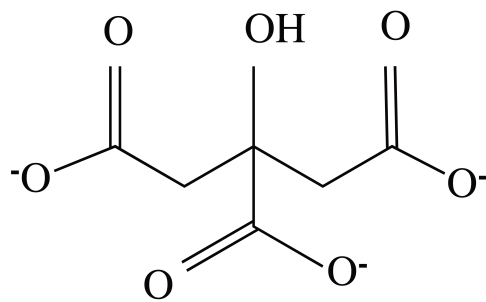
Figure 4. Size distribution of PVP-AgNPs and citrate-AgNPs at 5 mM NaNO₃ and pH = 7.0 ± 0.2

Table 3. Extent of silver ion dissolution at 5 mM NaNO₃ and pH = 7.0 ± 0.2

AgNPs	% Dissolution	Time (hour)	% Dissolution	Time (day)
PVP-AgNPs	0.050	0.5	0.70	7
AgNPs-HA	0.010	3.5	0.55	7
S-AgNPs	0.00014	5	0.032	7
S-AgNPs-HA	0.00010	5	0.030	7



PVP : $(\text{C}_6\text{H}_9\text{NO})_{360}$



Citrate : $\text{C}_6\text{H}_5\text{O}_7^{3-}$

Figure 5. Chemical structure of PVP and citrate

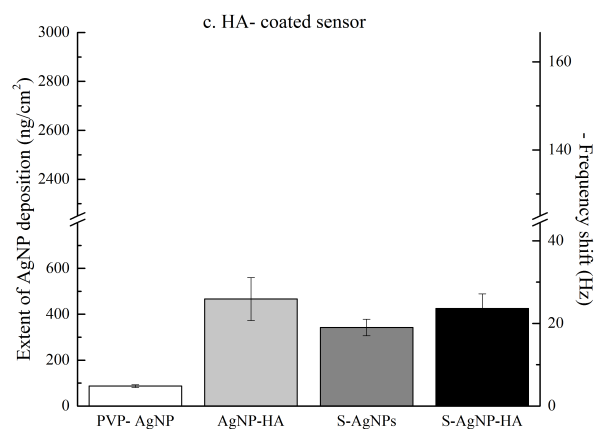
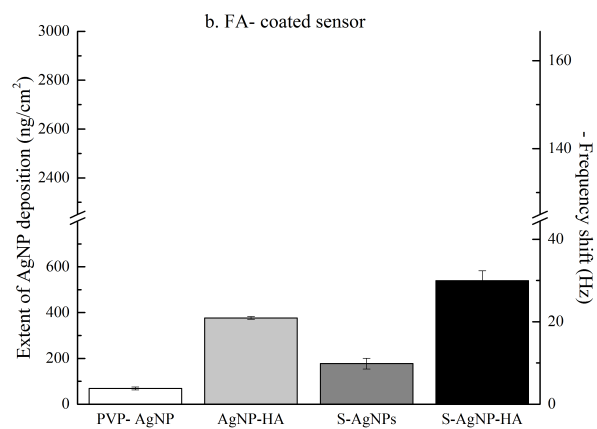
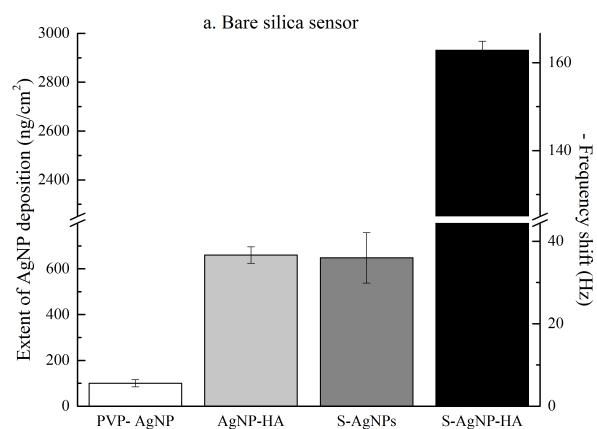


Figure 6. Extent of deposition of 4 types of AgNPs on three substrates: (a) Bare-silica (b) FA coated (c) HA coated at 5 mM NaNO₃ and pH 7.0 ± 0.2. Error bars are standard errors.

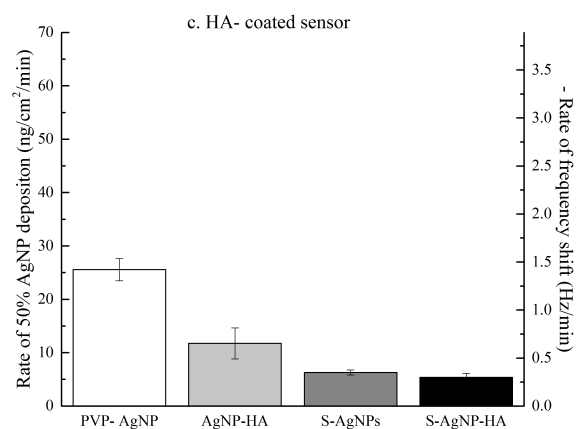
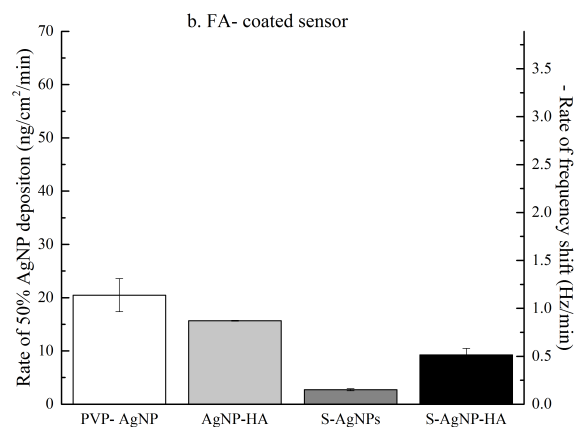
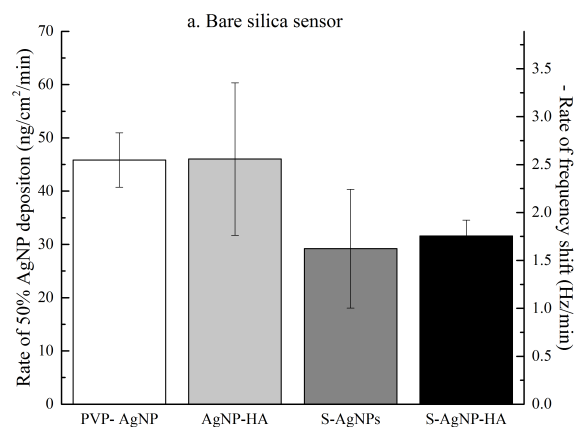


Figure 7. The rate of AgNPs deposition in terms of the time taken to reach 50% deposition on three substrates: (a) Bare-silica (b) FA coated (c) HA coated at 5 mM NaNO₃ and pH 7.0 ± 0.2. Error bars are standard errors.

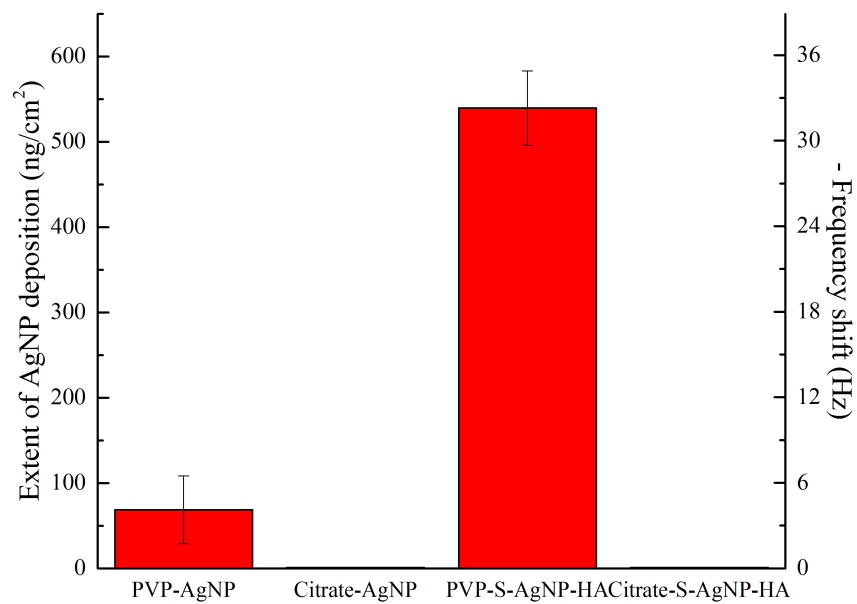


Figure 8. Deposition Extent of PVP and Citrate-coated AgNPs on FA coated substrates at 5 mM NaNO₃ and pH 7.0 ± 0.2. Error bars are standard errors.

Supplementary Information

for

Effect of Sulfidation and Natural Organic Matter
on the Deposition of Silver Nanoparticles

Table S1. One-tail T-test results of extent of AgNP deposition. Values in shaded cells mean not statistically different from each other ($p>0.05$)

P-AgNP on silica	AgNPs-HA on silica	S-AgNPs on silica	S-AgNPs-HA on silica	P-AgNP on HA	AgNPs-HA on HA	S-AgNPs on HA	S-AgNPs-HA on HA	P-AgNP on FA	AgNPs-HA on FA	S-AgNPs on FA	S-AgNPs-HA on FA	
/	0.018	0.0098	0.0022	0.51				0.17				P-AgNP on silica
	/	0.88	0.00050		0.021				0.023			AgNPs-HA on silica
		/	0.00010			0.022				0.010		S-AgNPs on silica
			/				0.0001				0.00001	S-AgNPs-HA on silica
				/	0.055	0.017	0.033	0.14				P-AgNP on HA
					/	0.32	0.74		0.44			AgNPs-HA on HA
						/	0.34			0.024		S-AgNPs on HA
							/				0.22	S-AgNPs-HA on HA
								/	0.0001	0.037	0.0074	P-AgNP on FA
									/	0.011	0.031	AgNPs-HA on FA
										/	0.0048	S-AgNPs on FA

Table S2. One-tail T-test results of rate of AgNP deposition. Values in shaded cells mean not statistically different from each other ($p > 0.05$)

P-AgNP on silica	AgNPs-HA on silica	S-AgNPs on silica	S-AgNPs-HA on silica	P-AgNP on HA	AgNPs-HA on HA	S-AgNPs on HA	S-AgNPs-HA on HA	P-AgNP on FA	AgNPs-HA on FA	S-AgNPs on FA	S-AgNPs-HA on FA	
/	0.44	0.15	0.022	0.0092				0.0034				P-AgNP on silica
	/	0.23	0.25		0.12				0.14			AgNPs-HA on silica
			0.43			0.14				0.13		S-AgNPs on silica
			/				0.029				0.026	S-AgNPs-HA on silica
				/	0.0094	0.019	0.020	0.13				P-AgNP on HA
					/	0.066	0.051		0.066			AgNPs-HA on HA
						/	0.26			0.033		S-AgNPs on HA
							/				0.023	S-AgNPs-HA on HA
								/	0.13	0.015	0.027	P-AgNP on FA
									/	0.000010	0.017	AgNPs-HA on FA
										/	0.016	S-AgNPs on FA
											/	S-AgNPs-HA on FA

Table S3. Two-tail T-test results of extent of AgNP deposition. Values in shaded cells mean not statistically different from each other ($p > 0.05$)

P-AgNP on silica	AgNPs-HA on silica	S-AgNPs on silica	S-AgNPs-HA on silica	P-AgNP on HA	AgNPs-HA on HA	S-AgNPs on HA	S-AgNPs-HA on HA	P-AgNP on FA	AgNPs-HA on FA	S-AgNPs on FA	S-AgNPs-HA on FA	
/	0.035	0.020	0.0045	1.02				0.35				P-AgNP on silica
	/	1.8	0.0010		0.042				0.046			AgNPs-HA on silica
		/	0.0002			0.045				0.020		S-AgNPs on silica
			/				0.0001				0.0001	S-AgNPs-HA on silica
				/	0.11	0.034	0.066	0.27				P-AgNP on HA
					/	0.63	1.5		0.88			AgNPs-HA on HA
						/	0.67			0.048		S-AgNPs on HA
							/				0.44	S-AgNPs-HA on HA
								/	0.0002	0.074	0.015	P-AgNP on FA
									/	0.021	0.062	AgNPs-HA on FA
										/	0.0095	S-AgNPs on FA
											/	S-AgNPs-HA on FA

Table S4. Two-tail T-test results of rate of AgNP deposition. Values in shaded cells mean not statistically different from each other (P>0.05)

P-AgNP on silica	AgNPs-HA on silica	S-AgNPs on silica	S-AgNPs-HA on silica	P-AgNP on HA	AgNPs-HA on HA	S-AgNPs on HA	S-AgNPs-HA on HA	P-AgNP on FA	AgNPs-HA on FA	S-AgNPs on FA	S-AgNPs-HA on FA	
/	0.88	0.30	0.044	0.019				0.0068				P-AgNP on silica
	/	0.46	0.49		0.2376				0.28			AgNPs-HA on silica
			0.87			0.28				0.25		S-AgNPs on silica
			/				0.057				0.052	S-AgNPs-HA on silica
				/	0.019	0.039	0.04	0.27				P-AgNP on HA
					/	0.13	0.10		0.13			AgNPs-HA on HA
						/	0.53			0.066		S-AgNPs on HA
							/				0.046	S-AgNPs-HA on HA
								/	0.26	0.029	0.054	P-AgNP on FA
									/	0.00010	0.035	AgNPs-HA on FA
										/	0.031	S-AgNPs on FA
											/	S-AgNPs-HA on FA

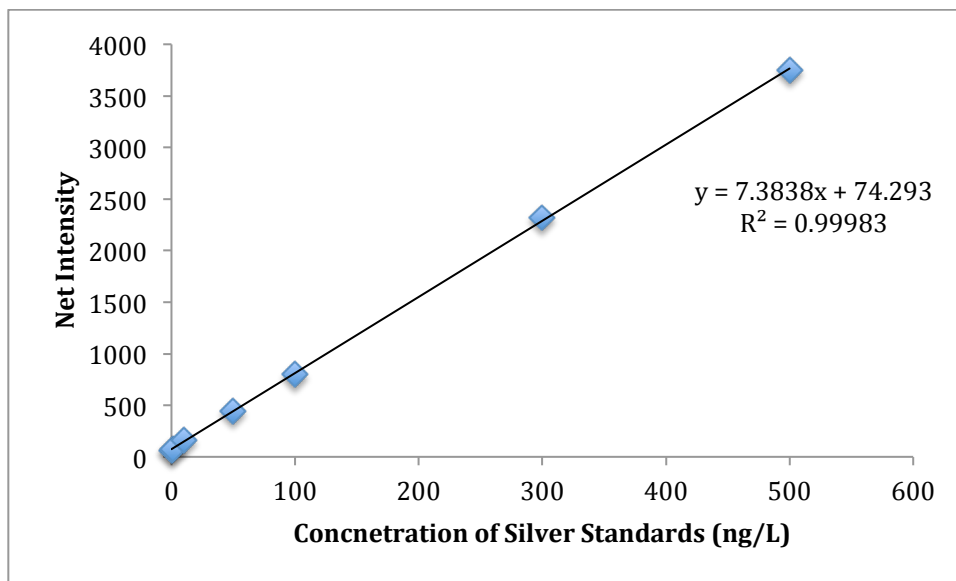


Figure S5. Calibration Curve of ICP-MS